Jozef Lebiedzik,[1] *Ph.D. and David L. Johnson,*[2] *Ph.D.*

Handguns and Ammunitions Indicators Extracted from the GSR Analysis

REFERENCE: Lebiedzik J, Johnson DL. Handguns and ammunitions indicators extracted from the GSR analysis. J Forensic Sci 2002;47(3):483–493.

ABSTRACT: The computer automated scanning electron microscope, X-ray microanalysis of Firearms Discharge Residue (FDR) can reveal substantial information about the circumstances of their generation beyond the presence of characteristic gunshot residue (GSR). Indicators of the type of weapon and ammunition used can be obtained from the distribution of GSR particle shapes and from the multi-element analysis of the FDR sample. This is demonstrated for a large database of GSR samples from nine different handguns and over 60 different ammunitions. An example classification scheme is presented for the supporting particles generally found present in FDR. When particle type area concentration ratios are normalized to the iron (Fe) particle type, results show it is possible to distinguish much about the metal used in the weapon manufacture, whether it was of large or small caliber, whether the bullets were jacketed or plated, and whether the cartridge cases were of aluminum, brass, or nickel-plated brass. Standardization of such analytical schemes would be advantageous.

KEYWORDS: forensic science, scanning electron microscopy, energy dispersive X-ray analysis, gunshot residue (GSR), firearms discharge residue (FDR), gunshot residue composition, automatic analyses, back scattered electron (BSE) signal, quantitative microscopy, image/X-ray analysis

Scanning electron microscopy (SEM) with X-ray microanalysis techniques of individual particle analysis (IPA) are employed by a large number of forensic laboratories world wide for the analysis of characteristic gunshot residue (GSR) particles. There is sufficient application of the methodology for ASTM to have introduced a standard (E 1588–95) (1), and Basu (2000) (2) indicates the technique is "uniformly accepted by the scientific community." Meng and Caddy (1997) (3) describe the advantages of the technique over bulk chemical analysis, but point out that its use is labor intensive and therefore best accomplished by automated procedures. Since the pioneering work of Keeley and Drayton (1981) (4), developments in automation for SEM-based IPA methods have advanced to become routine for GSR characterization.

Fully automated GSR analyses can save time by establishing an imaging threshold that skips over particles present from firearms discharge residue (FDR) that are not uniquely contributed by it (Germani, 1991) (5); (Lebiedzik and Johnson, 2000) (6). However, automation also makes it feasible to conduct analyses for more elements, beyond the requisite Pb, Ba, and Sb, as well as to gather and classify information on additional particle types (of lower average atomic number) that may be associated with FDR. Wallace and McQuillan (1984) (7) showed the value of a multi-element approach in distinguishing FDR from the particle assemblages generated by cartridge-operated industrial tools. Results of Wrobel, et al. (1998) (8) suggest the feasibility of separating ammunition types based on inclusion of additional elemental information; a concept further supported by the multi-element GSR study of Lebiedzik and Johnson (2000). The possibility that indicator particles originate from firing ammunition rounds is suggested by physics and chemistry; the process is a violent one. When the primer ignites the powder, (the propellant) in milliseconds the pressure increases inside the cartridge and the barrel to 15,000–40,000 PSI (9) depending on the ammunition. The high pressure and high temperature reaches about a melting point of lead, barium oxide, and antimony. The pressure also propels the oversized bullet through the rifled barrel cutting grooves into the bullet and forcing it into a spin. The deformation of the bullet to the exact profile of the barrel results in very high friction between the bullet and the barrel. Since the bullet exits the barrel at high velocities from 700–2000 fps, the friction at that velocity vaporizes part of the surface of the bullet and even picks up some particles from the barrel itself. This process, and the mechanical environment developed to contain and direct it, will affect the shape, type and chemical composition of the FDR produced. The resulting particle collection from the shooters hand or clothing may reveal some of the characteristics of the gun and the ammunition.

The present work advances the hypothesis that, under suitable analytical conditions, GSR analyses may carry additional information, derived from the larger suite of FDR particles, useful in describing some features of the gun and the ammunition that produced them. More than 60 different types of ammunition were fired under identical controlled conditions from nine carefully cleaned handguns. The weapon caliber ranged from .22LR to .44Mag. The shooter's hand was sampled for particles after firing a single round and after multiple rounds. Over 200 samples were collected and analyzed (2000 to 20,000 particles per sample). In addition to the automated analyses of the particles, specimens were examined by hand to study the morphology of GSR features. Working with this database, the pattern of ammunition and gun descriptors slowly emerged. These descriptors are based on elemental or compound concentrations of non-GSR particles and they can be found in abundance also on a non-shooter's hand. Therefore, they may be interpreted as such descriptors only in conjunction with GSR particles.

[1] Advanced Research Instruments Corp., 5151 Ward Road, Wheat Ridge, CO.

[2] Department of Chemistry, SUNY College of Environmental Science and Forestry, Syracuse, NY.

Received 7 May 2001; and in revised form 15 Sept. 2001; accepted 15 Sept. 2001.

Experimental Methods

Equipment

The SEM used in this work was ETEC Omniscan, product of ETEC Corp. equipped with a motorized stage, a product of Advanced Research Instruments (ARI) Corp. The X-ray analyzer consisted of an X-ray detector with a supporting electronics that is a product of KEVEX Corp. The multi channel analyzer (on a PC board) was from OXFORD Corp. The X-ray analysis software is an integral part of the image analyzer AutoSEM 1 produced by ARI Corp. The Back Scattered Electron Detector used (BSE) was also a product of ARI Corp.

Sample Collection and Analysis Conditions

All samples were collected immediately after firing of a carefully cleaned weapon via double-sided carbon based tape (SPI # 5072) cut to 8 mm in length and affixed to 1/2 in. diameter aluminum pin type SEM stubs. Each sample was acquired by ten impressions in different locations on the shooting hand. There was no additional sample preparation involved.

To eliminate previous history of fired ammunition, the barrel of each firearm was first scrubbed with a phosphor bronze brush and a patch soaked in Hoppe's No. 9 powder solvent. It was then electrochemically cleaned with "Outers Foul Out II Bore Cleaner" for lead and copper. The mechanism was again finished with the brush and soaked patches until the patches stayed clean. A visual inspection with a bright light source confirmed a mirror like finish. The cylinder of revolvers was cleaned in similar fashion, except for the electrochemical step. The outside of the guns was routinely wiped with a paper towel or a clean cloth soaked in a solvent, though the trigger mechanism was mostly ignored.

Each sample was analyzed at the same magnification (180 $\times$, 0.5 mm $\times$ 0.5 mm field of view) and the same operational settings. The analysis was performed on 10 $\times$ 10 fields, resulting in one hundred fields covering a 25 mm^2 area with a search resolution of 1024 $\times$ 1024 pixels. The pixel spacing of 0.5 μm guaranteed location of particles greater than this dimension.

The BSE signal was used for particle location and image analysis. The threshold for detecting particles via BSE signal was set to about atomic number 15 so that most of the particles detected were heavier than silicon. This generally eliminated clays, rutile, and rust particles from the dataset. The threshold was digitally maintained during analysis by the image analyzer to compensate for any long-term drift in incident beam intensity. The incident beam intensity is directly related to the threshold setting so; it is essential that it stay constant. Stabilization of the incident beam intensity is difficult and often ignored; we resolved this problem by digital threshold stabilization in the analyzer.

Routine SEM settings were: 20 kV accelerating potential, absorbed current on carbon tape set to 1 nA, and a working distance of 20 mm. Sample tilt was set to zero and confirmed by focus on different and extreme positions on the sample. X-ray acquisition was set to 5 s "live time" or 5000 counts, which ever was reached first. The position of the chisel nose detector was set to produce 40–50% dead time on an iron standard. All of the analyses were performed unattended because of the length of the time required. The average time of analysis can be estimated to be 2–4 s per particle for a typical sample. For an average sample with about 10,000 particles, this translates to about to 10 h; the actual time of analysis was proportional to sample loading. The number of particles analyzed per sample was typically between 2000–20,000.

Quantitative Microscopy Analysis

If an SEM/EDX technique searches only for X-ray signals from the traditional characteristic elements, Pb, Ba, and Sb, their qualitative presence is sufficient for the expert analyst to determine the presence or absence of GSR. When additional elements are monitored, the results need to be interpreted from the perspective of X-ray microanalysis as opposed to quantitative X-ray analysis. While both analyses measure composition as percentages, or parts per million, they are based on different implementations of X-ray emission spectroscopy. We refer to quantitative microscopy analysis as IPA/SAX (Individual Particle Analysis by Scanning electron microscopy with Automated image analysis and X-ray microanalysis). The technique not only measures the feature image morphological parameters of size and shape, but also performs rapid X-ray analysis on each particle. Quantitative results are obtained for the number and projected area of individual particles (and particle types) per unit area of specimen characterized. In contrast, quantitative X-ray analysis is generally applied to polished flat specimens whose bulk phase chemical analysis is to be determined, employing long X-ray count times and ZAF corrections.

For the present research, X-ray data were gathered for 23 (energy) regions of interest (ROI) for K_α and L_α or L_β X-ray lines from 21 elements. Two L series lines were monitored for Sb and for Ba to help insure accuracy of identification. Background corrections were applied from counts in the two channels left and right of the ROI. An element presence test of at least 95% confidence was applied; net counts were required to be at least 2 square roots above background. The relative X-ray intensity was computed for each ROI and used with specific upper- and lower-bound criteria for each element to classify observations into particle types.

All of the concentration ratios shown in figures for results (below) are relative to iron. X-ray analysis is used only to tag each particle as a specific compound. Then, the concentration of a given compound is calculated as projected total area of all particles of the same type to the total scanned [searched] area. This is defined by the equation:

Stainless steel concentration [area fraction] for "n" particles

$$SS = \frac{\sum_{i=1}^{n} A_i \; ss}{\text{Searched area}}$$

The significance of the concentration defined by an area fraction above is several fold: it takes into account sizes of particles as well as count or population; it is independent of other particle types found in the same sample; and, it is independent from the threshold setting (within some limits).

Particle Classification Procedure

In Appendix I to this report, we present the detailed classification criteria used in our study. It consists of a fixed set of element relative X-ray intensity ranges arranged as a linear sorting algorithm. As such, it is a "first fit" sorting scheme. During data summary, the relative X-ray intensity for each of the 23 ROI is computed (for each particle) and compared with the list of classification criteria. The observations are classified as belonging to the first particle type for which all criteria are satisfied. The class definitions we present have been developed by inspection, through an iterative process over the course of the study. Note that the GSR category requires both Sb and Ba, but does not require Pb to be present; this is consistent with the ASTM Standard E1588–95 definitions.

The sorting algorithm uses three kinds of X-ray relative intensity criteria: 1) **inclusive**, 2) **exclusive**, and 3) **allowable** limits. Suppose a particle analyzed had the following X-ray relative intensity composition: Fe=30%, Pb=20% and the ROI's for Sb1, Sb2, Cr, K and Mg each showed 10% of the net X-ray count, with all other RIO's showing no X-ray contribution. The *inclusive* criteria for the GSR class require that both Sb and Ba be present, so the algorithm searches the next class—Antimony. Here, the *allowable* requirement for Fe is that it must be less than 20%, the same criterion as shown for the Pb+Sb class. In similar fashion, it can be observed that for the example particle Stainless Steel is the first category for which all classification criteria are met, and the observation will be so designated. Note that the *exclusive* criterion of Cr<10% prevents the example particle from being classified in the Iron category just above Stainless Steel.

The classification criteria we show in Appendix I are specific to the instrumental system we employed; they are empirical and are presented for completeness of interpreting the results we obtained. The X-ray relative intensity composition of the particles present in FDR will be somewhat sensitive to the ways in which elemental ROI's are established, how background counts are determined for calculation of total net counts, and the instrument-specific details of how element overlap corrections are carried out. The general results we have obtained will be reproducible on other analytical systems, but details of the exact particle classification may not translate.

Note that in the results presented below findings are summarized by the ratio of particle types found. Furthermore, the total (projected) area fraction contributed by the particle types is used, not simply the number of particles of each type. This approach helps dampen the variability in FDR deposits that occur in both the generation and sampling processes.

Results and Discussion

Morphology Differences in Unique GSR Features

The most easily recognized characteristic of many GSR particles is their spherical shape, a form consistent with a high temperature molten phase. The frequently cited Aerospace Report (Wolten et al., 1977) (10) states "70–100 percent of the unique particles in a sample of GSR are spheroidal." Basu (1982) (11) reports three types of GSR particles: 1) spheroids, 2) irregular, and 3) Ba+Sb particles with lead layer. Our experience indicates, that his third category may be included with the spheroids as less than perfect spheroid forming particles. Schwoeble and Exline (2000) (12), in their recent excellent publication, acknowledged two basic morphologies of GSR particles, but nevertheless stated, in part, "GSR particles are generally spherical in shape." Our extensive examination indicates that the tendency to form spheroids is related to the type of ammunition fired. Although direct study of the GSR particle formation process is beyond the scope of this work, it is not too difficult to consider the basics. The temperature and pressure in the barrel are function of propellant, primer, and the length of the barrel. All, except the barrel length are properties of the ammunition.

The morphology of unique GSR particles can be divided into three basic categories:

1. Spheroid forming. Most of the GSR particles are formed from a liquid state; if not a spheroid, they are at least well rounded features.
2. Irregular shapes. These are fractured or partially sintered particles; GSR in this category shows a scarce presence of spheroids.
3. A combination of the two types above. GSR from most ammunition studied falls into this group, but with a variety of proportional mixes.

Figures 1*a,* 1*b* and 2*a*, 2*b* are BSE images of GSR particles without any sample preparation. The bright spots are lead or lead-antimony rich areas. Each photomicrograph features a micron marker on the left side of the legend.

Figures 1*a* and 1*b* illustrate unique GSR that tends to form spheroids. The ammunition category that generated these features includes: 9 mm FMJ Chinese Norinco, Russian TCW, and Czech Republic Sellier&Bellot; only about 20% of the GSR particles showed non-spheroid forming tendency. Figures 2*a* and 2*b* illustrate typical non-spheroid formation of GSR particles. This category includes: .45 ACP Black Talon, 9 mm Mag. Safe, .45 ACP JHP Winchester and .45 ACP Hornandy. There may be only 10% of particles found to be spheroid in form. These two typically distinct categories based exclusively on the morphology of GSR particles include only a few types of ammunitions.

The above illustrations are representative of a much larger collection of particles.

Handgun Descriptors

Using the classification scheme developed for FDR, we looked at the ratios of various possible indicator particle types. At least three different types of handguns can be distinguished from the quantitative analysis of GSR supporting particles. A high stainless steel to iron ratio (SS/Fe) indicates stainless steel handgun, as is illustrated in Fig. 3. By comparison, a low SS/Fe ratio indicates carbon steel handgun; a substantially higher ratio is found for a stainless steel gun than a carbon steel gun. Results are shown for these handguns after a variable number of rounds had been discharged. A single round does not always produce higher SS/Fe ratio due to a higher statistical error although it does in most cases. After 10 to 20 rounds, we observed a consistently higher stainless steel to iron ratio.

Figure 4 shows that in a similar fashion, the titanium to iron (Ti/Fe) ratio can point to the firing of a titanium weapon. Here, a titanium revolver was compared with several other handguns; the titanium particles from the Taurus 357 Magnum Tracker showed a dramatic increase. The amount of titanium particles in other handguns is negligibly small in comparison to the titanium revolver. Note the increase of titanium when more than one round is fired. The relative area ratio of titanium to iron particles computed is a better concentration indicator than a simple particle count. It is useful to be familiar with the variety of ways handguns are constructed to be able to successfully interpret the data. For example: The Taurus 357 Magnum Tracker revolver is a titanium gun, but has a stainless steel barrel liner resulting in high stainless steel to Iron ratio and at the same time also high titanium concentration.

Ammunition Type Indicators

A number of significant ammunition descriptors can be found from quantitative analysis of the GSR supporting particles, or firearms discharge residue characterization. For example, a high lead concentration, or to be more specific a Pb/Fe area ratio greater than 1.0, is indicative of a lead bullet. This includes several plated .22LR bullets; plating on the .22LR bullets is so thin that the lead core dominates the picture. With respect to weapon caliber and bullet type, we found in samples collected after the

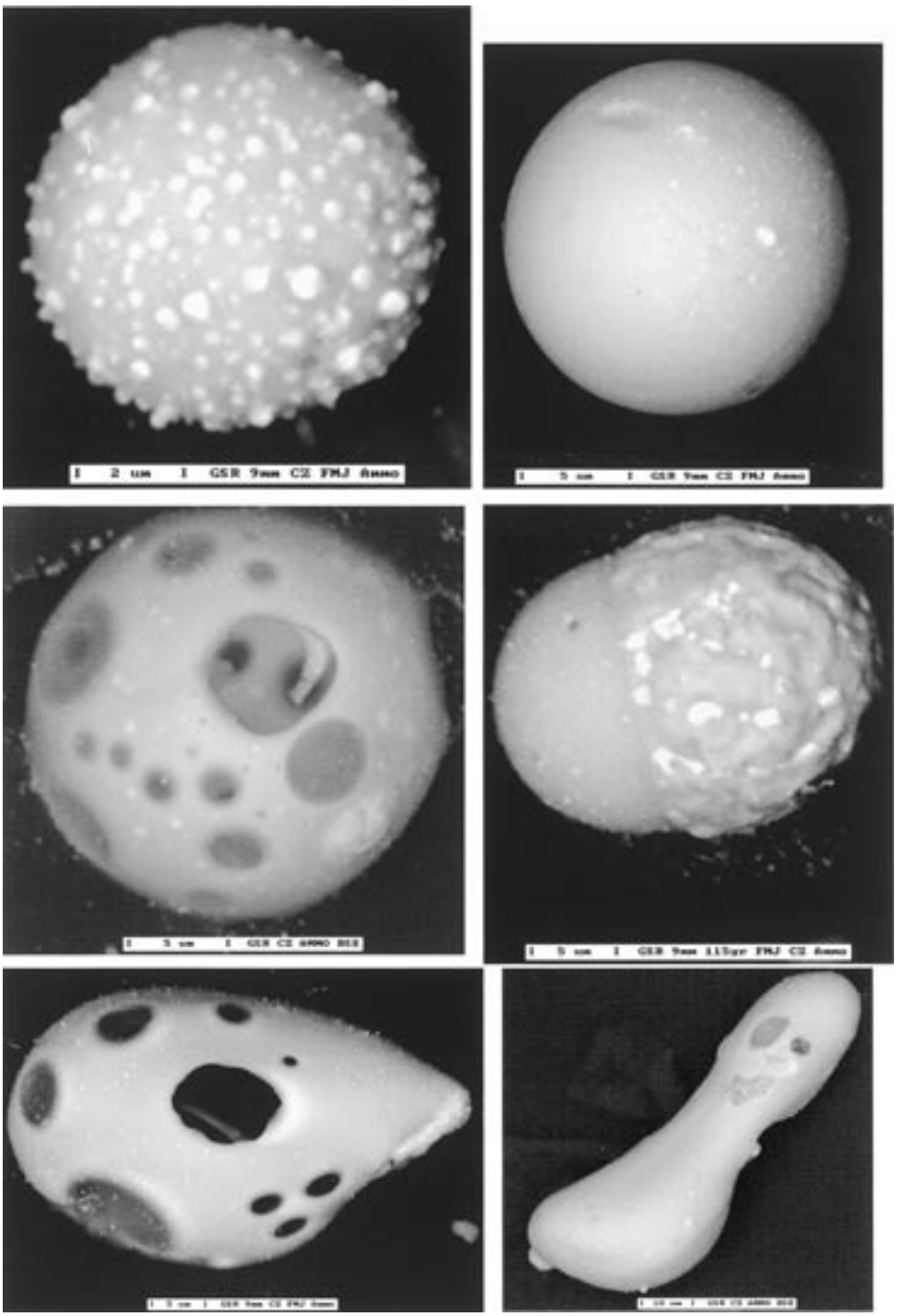

FIG. 1a—*Typical spherioid forming GSR.*

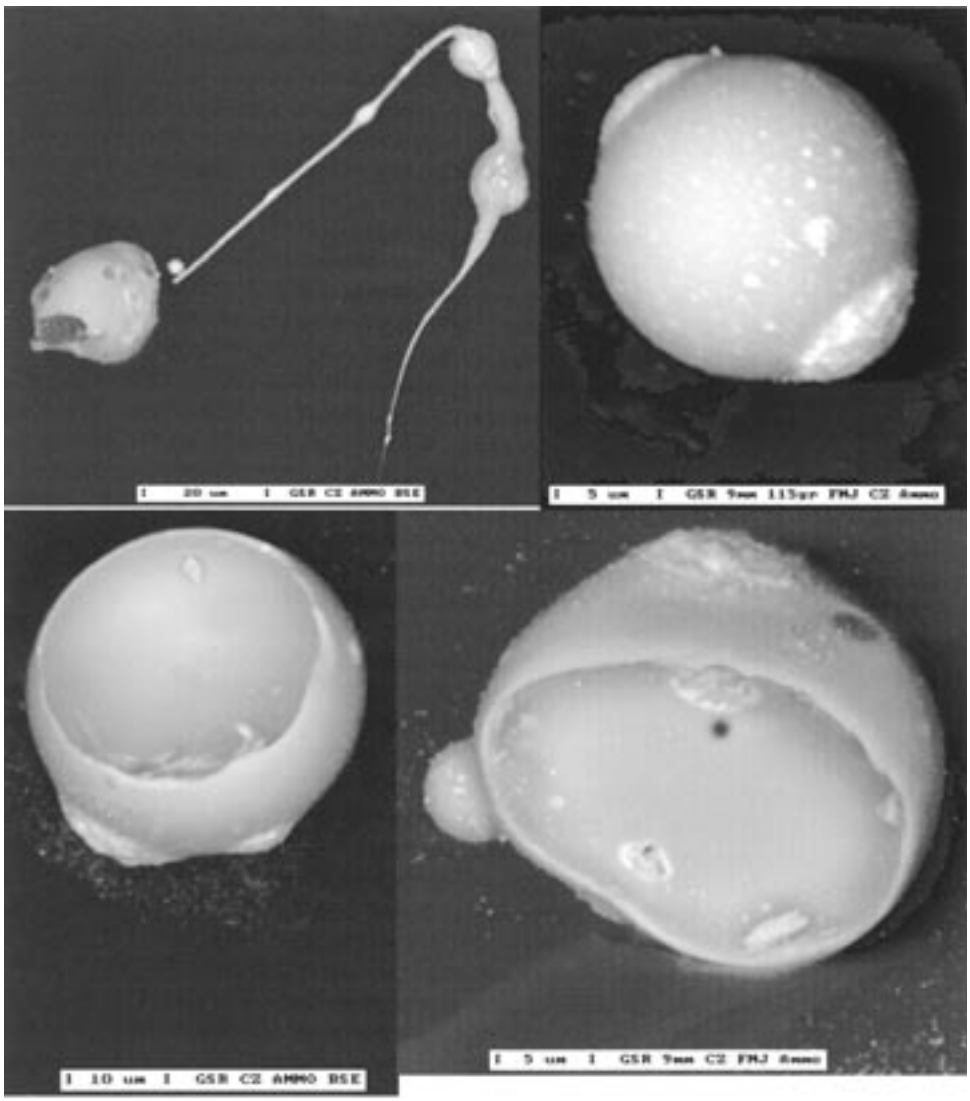

FIG. 1b—*Typical spheroid forming GSR.*

discharge of 20 rounds, that:

- An Pb/Fe>100 is associated with caliber higher than .22LR
- If the Pb/Fe <100 but >1, it is most likely .22LR
- An Pb/Fe <1 indicates a jacketed bullet of caliber > .22LR

Figure 5 illustrates the high Pb/Fe concentration (middle of the plot) after 20 rounds each of two different caliber ammunition. For comparison, data from a .38 Special (+P+ Con-Bon 158gr LHP) showed a Pb/Fe ratio of 260 after analysis of 22,758 lead particles.

The first three sets of bars correspond to .22LR bullets, while the two very short ones belong to jacketed 9 mm bullets. The thick copper jacket of the typical 9 mm bullet prevents direct contact between the lead core and the barrel of the gun, resulting in very little production of lead particles. The brass or copper plating of the 22LR bullets on the other hand, has little effect on the lead concentration and reduces the Pb/Fe value to about half of the lead bullet. The plating is so thin that for all practical purposes we can treat the bullet as a lead one. However, monitoring the PbCu/Fe and Pb-Brass/Fe ratios may provide the ability to distinguish a copper plated bullet from brass plated one.

The plating of a lead bullet may be determined by looking at several other indicators. An extremely high brass to iron ration alone would point to brass plated lead bullet; the ratio in Fig. 5 for the .22LR brass plated bullet is 67.5. The lead+brass/iron value for brass plated lead bullet is also very high in comparison to any other bullet. The copper plated bullet is not so obvious from this illustration. The safest way to deduce a copper plated bullet is mostly by default. A high lead-copper/iron ration indicates a plated bullet. An absence of very high brass/Fe ratio as well as Pb-brass/Fe points to the only one left, a copper plated lead 22LR.

The Cartridge Case

The most popular cases are made of brass, and the second most popular cases appear to be nickel-plated brass. Aluminum and steel cases are also employed. Aluminum case may be easily determined from a high relative concentration of aluminum. The steel case is difficult; we were unable to find a reliable steel case indicator. Dis-

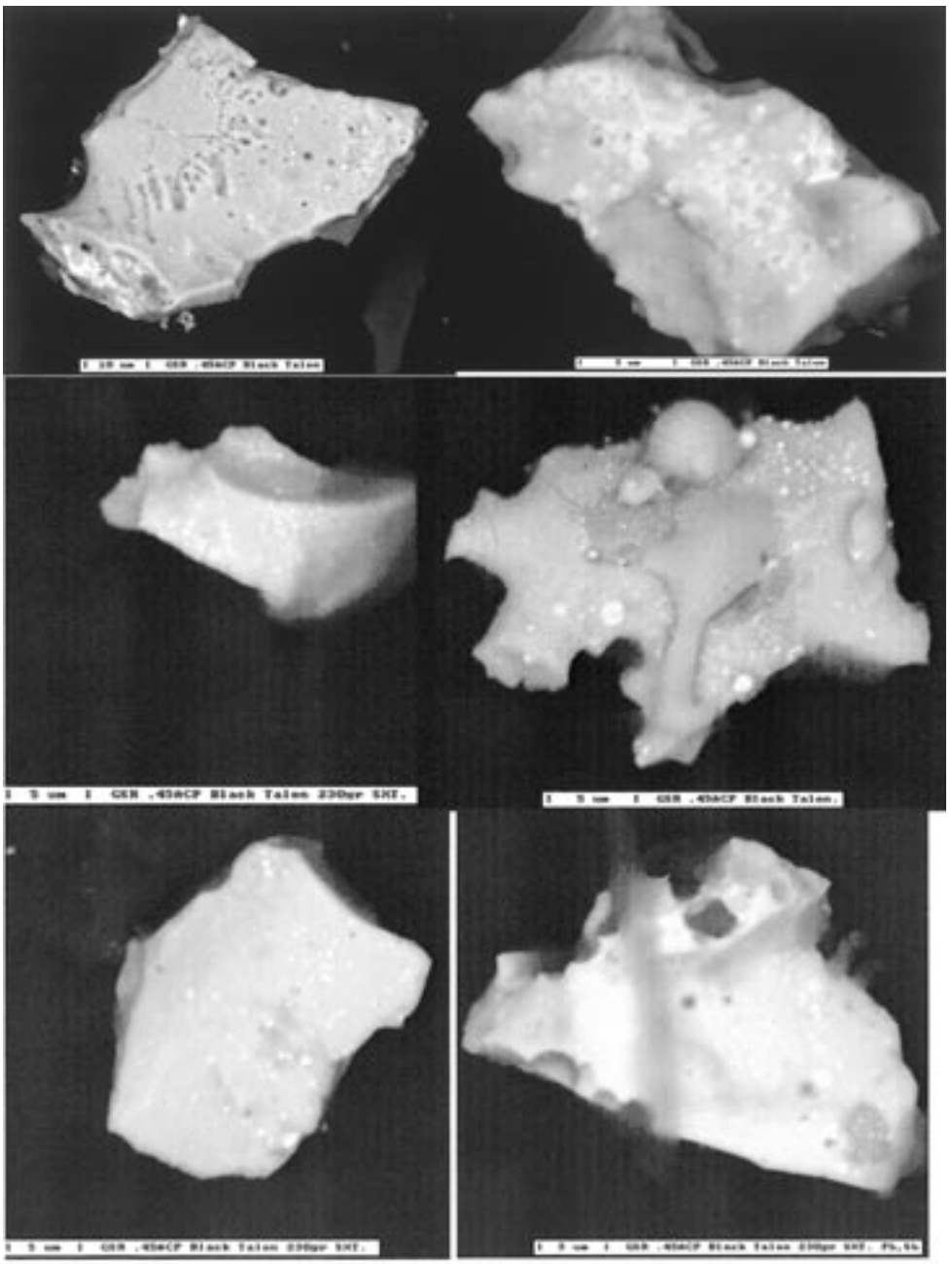

FIG. 2a—*Non-spheroid forming GSR.*

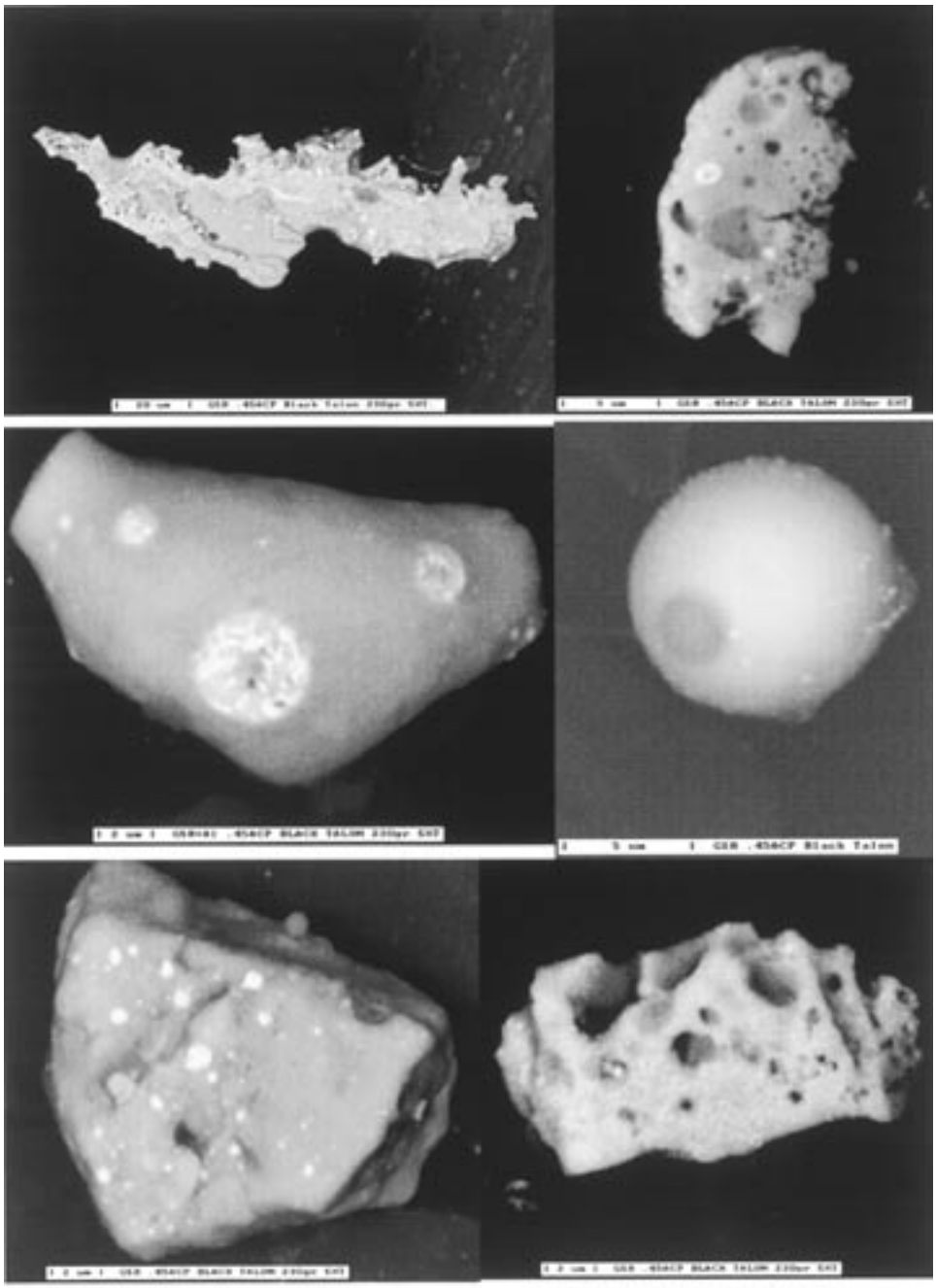

FIG. 2b—*Non-spheroid forming GSR.*

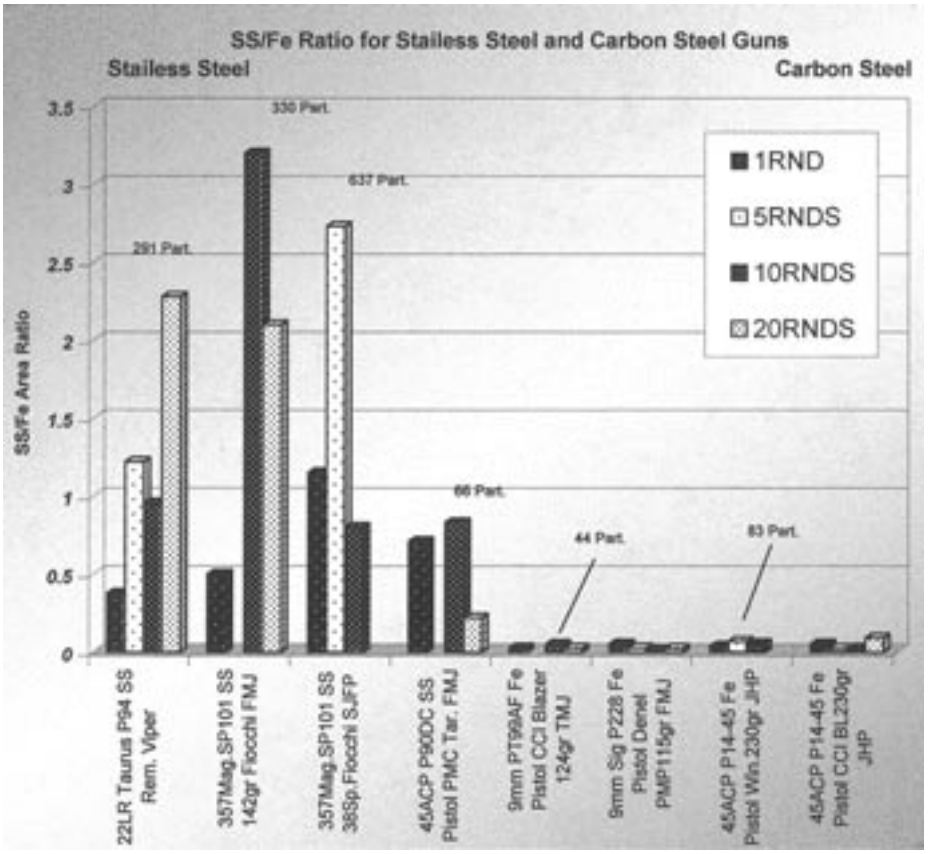

FIG. 3—*Comparison of stainless steel guns to carbon steel.*

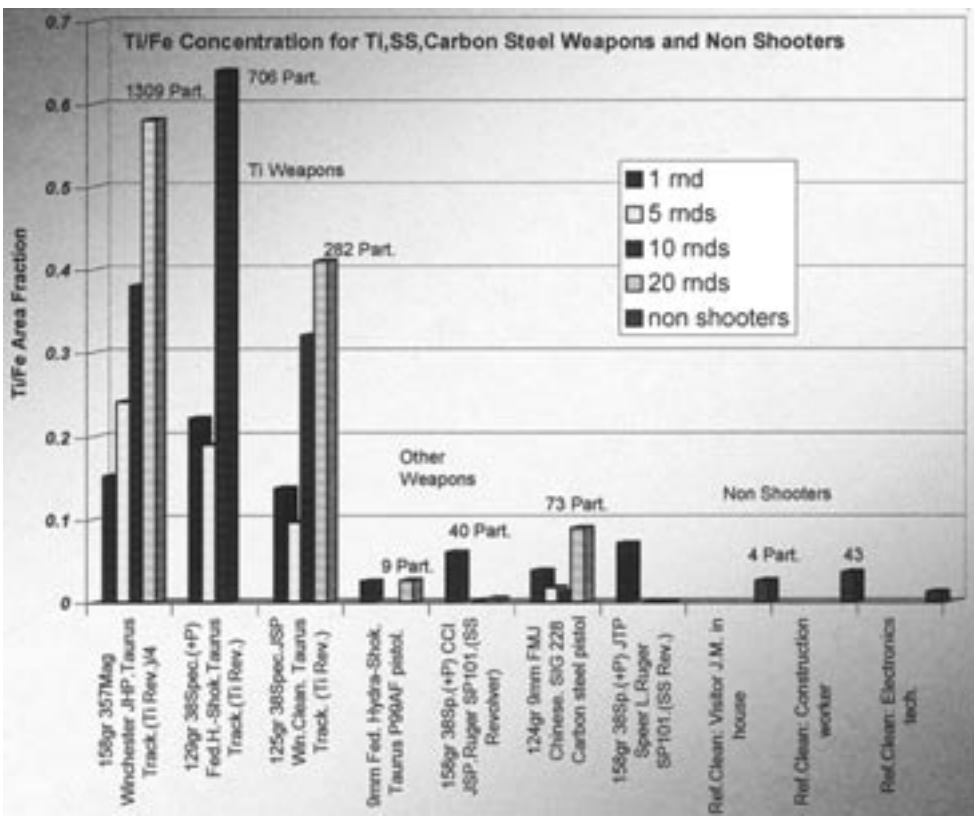

FIG. 4—*Relative titanium concentionation from titanium revolver in contrast to other firearms. First three sets belong to the titanium revolver.*

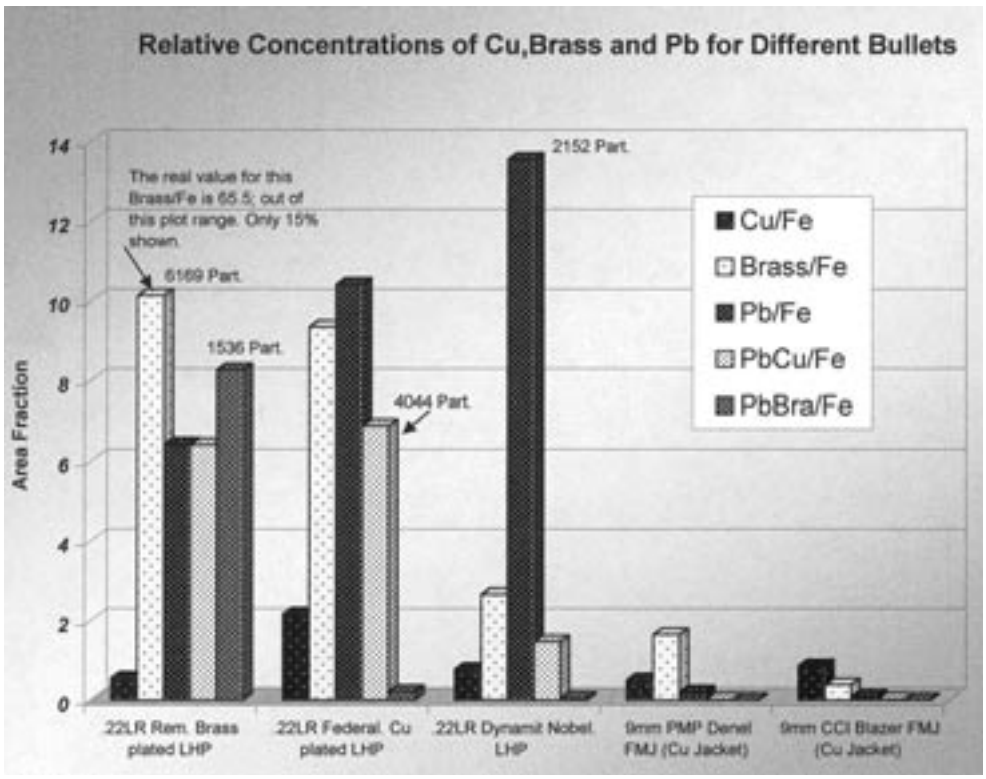

FIG. 5—*High relative concentration of bullet plating material reveals the type of plating. Some of the brass particles originate from the casing. Note the lack of brass for the 9 mm CCI Blazer that features aluminum casing.*

tinguishing between the top two cases is straightforward. A simple indicator of whether a brass or a nickel-plated brass cartridge was a part of the ammunition fired, is the nickel to iron ratio. Figure 6 illustrates the contrast between the two types of cases.

In a rare case, the higher nickel to iron ratio may be misleading. Since we cannot determine the origin of the nickel particles, the nickel-plated case is only a "most likely origin." An older 9 mm FMJ Luger by Sellier&Bellot from the Czech republic features a nickel-plated bullet and brass case details of which are shown in Figs. 7 and 8.

While (apparently) not presently available with this kind of bullet, this ammunition produced Ni/Fe values between 1.5, for a single round, and 2.3 for multiple rounds. A typical nickel-plated brass cases produced Ni/Fe values below 1.0, as in Fig. 6. The unusually high plating material concentration is similar to other plated bullets as can be seen from Fig. 5. This high concentration may be an indicator that the nickel particles originated from the bullet instead from the case.

Limitations and Applicability

The above results were obtained under carefully controlled conditions that would not necessarily apply to a sample collected many hours after the shooting unless the conditions were well preserved and enough particles were collected. The above data also illustrate that when more rounds of the same ammunition are fired, more of the relevant particles are collected, since the contaminated gun produces far more particles than a clean one. This fact points to the practical aspect of this approach since a suspect is more likely to use the same ammunition for practice than a variety of ammunitions. Assuming that gunmen tend to clean their guns superficially, a continuity of ammunition history would enhance the data. This work illustrates possibility of extending the usefulness of GSR and other particles collected from the shooter's hand. The indicators can point to the type of material used for firearm fabrication, and to a (albeit limited) description of the ammunition. These research results pertaining to firearms discharge residue support the efforts of Wrobel, et al. to establish a descriptive database for use in criminal investigations.

The major limitation for this type of inquiry is mostly in the statistics. Interpretation becomes easier as more shots are fired and less time is allowed for particles to be removed prior to sampling, and when the ammunition used is consistent with previous firings. If methods were available for standardizing the analytical protocol, it would be possible, through the sharing of results, to build the sort of database envisioned by Wrobel, et al. There are theoretical approaches that could be employed if agreement could be reached on precisely which elements to monitor. Our own research is continuing with the use of multi-element particulate standards of known bulk composition to develop an a priori method for designating elemental regions of interest and background and overlap corrections. We hypothesize that obtaining accurate inter-element atomic ratios in the summary of X-ray relative intensities, two different analysis systems can be made to give the same results in the characterization of FDR.

Conclusions

Different ammunition/weapon combinations produce different particle assemblages for the deposit we know as firearms discharge residue. This results from chemical variation in the ingredients of the primer and powder in the ammunition from different manu-

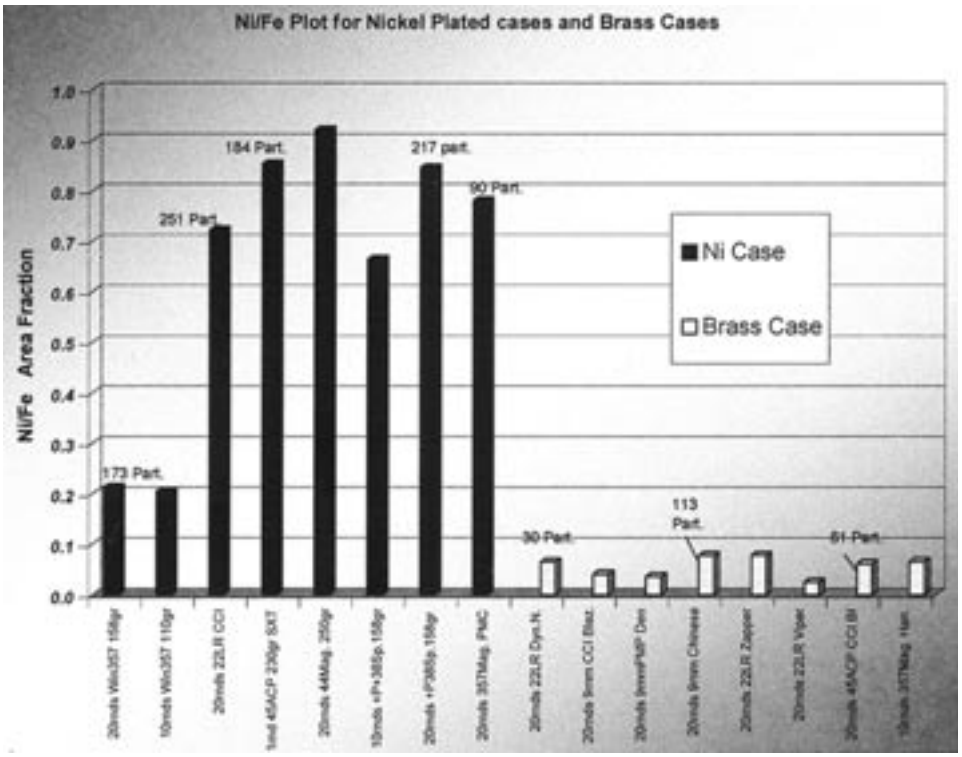

FIG. 6—*High nickel to iron ratio indicates a nickel-plated case.*

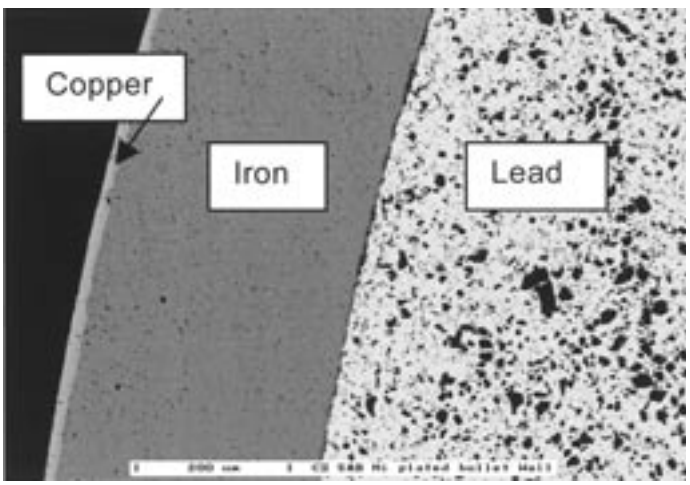

FIG. 7—*Cross-section of a 9 mm FMJ Sellier&Bellot bullet. BSE image. The lead core is surrounded with 340 micron iron jacket and 15 micron copper layer. The nickel plating is not visible at this magnification. The width of the photomicrograph is 900 μm.*

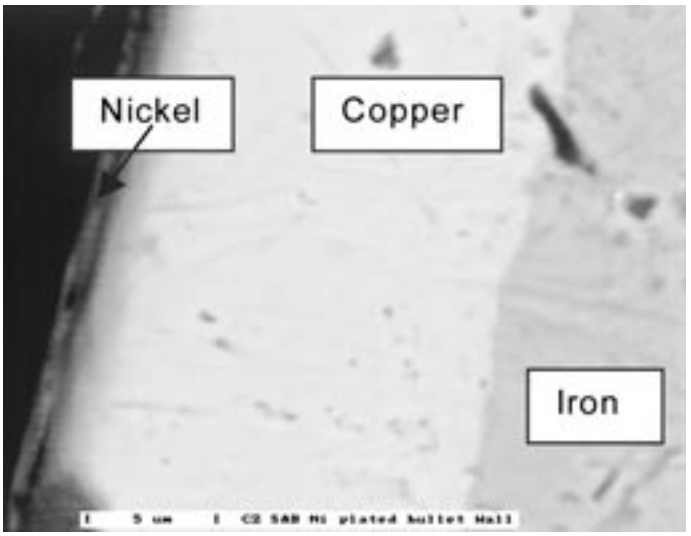

FIG. 8—*Thirty times higher magnification of the same location as in Fig. 7. The Nickel plating, only about half micron is visible on the left. The width of the photomicrograph is 30 μm.*

facturers, the metals used for fabrication of the bullets and the cartridge cases, and from the metallurgy of the weapon firing the ammunition.

To some extent, these differences can be observed simply from the morphology of the GSR particles. Many of them are not spherical in form, and the distribution of shape types depends upon the particular ammunition fired.

If a multi-element approach is taken in the IPA/SAX techniques for GSR, and a BSE threshold is established that allows analysis of metal particles lighter than Pb, Ba, and Sb, then the additional characteristic information above becomes available to the analyst.

Results here show that, under ideal conditions, one can distinguish between guns made of stainless steel, carbon steel and titanium; can learn about the caliber of the weapon from the Pb/Fe ratio; can determine information about the plating or jacketing of the bullets; and can discern whether the cartridge cases used were aluminum, brass, or nickel-plated brass.

In a case, when a variety of ammunition is fired, the ammunition

Appendix

Chemical Classification Scheme used in this research. Limits are based on relative x-ray intensity (% of Net Counts)

	Na	Mg	Al	Si	P	S	Cl	K	Sb1	Sb2	Ba1	Ba2	Cr	Mn	Fe	Co	Ni	Cu	Zn	Pb
GSR	<30	<50	<50	<50	<50	<50	<40	<40	3~80	2~70	5~90	3~80	<50	<50	<50	<50	<50	<80	<50	<80
Antimony	<30	<40	<40	<30	<30	<65	<45	<35	10~99	4~80	<25	<5	<20	<20	<20	<20	<20	<50	<20	<35
Barium	<20	<40	<55	<75	<30	<20	<30	<50	<50	<30	10~99	3~90	<20	<20	<30	<20	<35	<50	<30	<20
Pb + Sb	<20	<20	<20	<30	<20	<20	<30	<20	10~90	4~80	<20	<20	<20	<20	<20	<20	<20	<20	<20	15~80
Pb + Ba	<20	<20	<20	<30	<20	<20	<35	<20	<30	<30	10~90	3~80	<20	<20	<30	<20	<20	<40	<20	15~80
Magnesium	<20	20~99	<40	<25	<20	<30	<20	<20	<20	<2	<10	<25	<20	<20	<25	<20	<20	<30	<30	<20
Aluminum	<20	<25	30~99	<40	<50	<40	<35	<20	<20	<20	<20	<20	<20	<20	<50	<20	<20	<40	<20	<25
Silicates	<20	<80	<50	24~99	<55	<50	<40	<50	<45	<35	<45	<30	<30	<40	<50	<45	<30	<50	<35	<35
Sulfur	<25	<20	<36	<45	<30	30~99	<30	<50	<40	<20	<40	<20	<30	<20	<50	<20	<20	<30	<40	<20
Chlorine	<5	<40	<35	<40	<20	<35	30~99	<30	<20	<20	<20	<20	<20	<20	<20	<20	<20	<30	<20	<35
Potassium	<20	<20	<20	<30	<20	<20	<20	30~99	<10	<5	<20	<5	<20	<20	<20	<20	<20	<30	<20	<20
K + Cl	<20	<20	<20	<20	<20	<30	20~70	20~70	<20	<20	<20	<20	<20	<20	<20	<20	<20	<30	<20	<25
Na + Cl	5~80	<20	<20	<20	<20	<20	30~95	<20	<10	<10	<20	<20	<20	<20	<20	<20	<20	<30	<20	<25
Calcium	<20	<20	<20	<20	<20	<40	<20	<30	35~99	<10	<20	<2	<20	<20	<20	<20	<20	<30	<20	<35
Iron	<20	<45	<45	<40	<45	<40	<50	<40	<30	<20	<40	<20	<5	<30	30~99	<10	<10	<30	<40	<25
Stainless St.	<20	<40	<40	<40	<20	<30	<20	<20	<50	<30	<30	<30	5~50	<40	20~99	<40	<50	<20	<30	<30
Fe + Ni	<20	<20	<20	<20	<20	<20	<20	<20	<10	<2	<20	<2	<5	<20	30~99	<20	5~90	<30	<20	<20
Fe + Cr	<20	<20	<20	<30	<20	<30	<20	<20	<10	<2	<20	<2	10~80	<20	20~90	<20	<20	<30	<20	<20
Cobalt	<20	<20	<20	<20	<20	<20	<20	<20	<10	<2	<20	<2	<20	<20	<20	40~99	<20	<30	<20	<20
Nickel	<20	<20	<20	<35	<35	<20	<20	<20	<10	<2	<20	<2	<30	<20	<20	<20	<30~99	<30	<20	<20
Cu + Ni	<20	<20	<35	<20	<20	<20	<20	<20	<10	<2	<20	<2	<20	<20	<20	<30	5~80	20~80	<5	<20
Copper	<20	<55	<35	<40	<20	<60	<40	<55	<40	<20	<40	<20	<20	<40	<40	<20	<20	30~99	<2	<10
Zinc	<20	<20	<20	<40	<50	<20	<40	<20	<20	<20	<40	<20	<20	<20	<45	<20	<20	<35	30~99	<20
Lead	<25	<40	<40	<60	<55	<25	<50	<65	<40	<30	<50	<30	<35	<25	<50	<25	<25	<20	<35	10~99
Cu + Pb	<20	<20	<25	<30	<20	<40	<40	<30	<30	<20	<35	<20	<20	<20	<25	<20	<20	20~95	<2	10~80
Brass + Pb	<20	<40	<40	<40	<20	<30	<20	<20	<50	<30	<30	<30	<20	<20	<20	<20	<30	20~90	2~80	10~80
Pb + Al	<20	<20	30~80	<20	<20	<20	<20	<20	<30	<20	<30	<20	<20	<20	<20	<20	<20	<20	<20	20~80
Brass	<20	<20	<30	<40	<20	<30	<45	<30	<30	<20	<30	<20	<20	<20	<30	<20	<4	30~95	2~80	<20
Brass + Ni	<20	<40	<40	<40	<20	<30	<20	<20	<50	<30	<30	<30	<20	<20	<20	<20	4~50	30~90	5~60	<30
Titanium	<20	<20	<30	<55	<30	<60	<30	<40	<20	<20	35~90	<2	<20	<20	<40	<20	<30	<30	<20	<20

descriptive indicators will be difficult to interpret due to the combined influence of more than one type of ammunition. However, the weapon material indicators will be unaffected by the variety of ammunitions.

The general utility of this type of analysis would be enhanced if different analytical laboratories could exchange results, increasing the potential for probative value. This might be accomplished if a suitable degree of standardization could be brought to bear on the analytical conditions.

Acknowledgments

The authors are grateful to the Boulder Rifle Club for providing the shooting facilities.

References

1. Designation E 158895. Standard guide for gunshot residue analysis by scanning electron microscopy/energy-dispersive spectroscopy. Annual Book of ASTM Standards. American Society of Testing and Materials. West Conshohocken, PA 1995.
2. Basu S. Scanning electron microscopy in forensic science. In: Encyclopedia of Analytical Chemistry, Meyers, RA, editors. J Wiley & Sons, Chichester, UK 2000.
3. Meng HM, Caddy B. Gunshot residue analysis—a review. J Forensic Sci 1997;42(4):553–70.
4. Keeley RH, Draton WB. Automatic particle analysis with the SEM. J Forensic Sci 1981;21(2):115–6.
5. Germani MS. Evaluation of instrumental parameters for automated scanning electron microscopy/gunshot residue particle analysis. J Forensic Sci 1991;36(2):331–42.
6. Lebiedzik J, Johnson DL. Rapid search and quantitative analysis of gunshot residue particles in the SEM. J Forensic Sci 2000;45(1):83–92.
7. Wallace JS, McQuillan J. Discharge residues from cartridge-operated industrial tools. J Forensic Sci 1984;24:495–508.
8. Wrobel HA, Millar JJ, Kijek M. Identification of ammunition from gunshot residues and other cartridge related materials—a preliminary model using .22 caliber rimfire ammunition. J Forensic Sci 1998;43(2): 324–8.
9. Lyman Products Corp. Pistol and Revolver Reloading Handbook, Second Addition 1997.
10. Wolten GM, Nesbitt RS, Calloway AR, Loper GL, Jones PF. Final report on particle analysis for gunshot residue detection. The Aerospace Corp., El Segundo, CA. 1977;ATR-77 (7915)-3.
11. Basu S. Formation of gunshot residues. J Forensic Sci 1982;27:72–1.
12. Schwoeble AJ, Exline DL. Current methods in forensic gunshot residue analysis. CRC Press LLC, 2000 N.W. Corporate Blvd., Boca Raton, Florida 33431. 2000.

Additional information and reprint requests:
Jozef Lebiedzik
Advanced Research Instruments Corp.
5151 Ward Road
Wheat Ridge, CO 80033